Barbara Koscielniak, Grzegorz Smola*, Zbigniew Grzesik and Adam Hernas

Oxidation Resistance of Austenitic Steels under Thermal Shock Conditions in an Environment Containing Water Vapor

DOI 10.1515/htmp-2016-0209
Received September 26, 2016; accepted January 28, 2017

Abstract: The oxidation behavior of Super 304 H, Sanicro 25, HR3C and HR6W steels, which are recommended for use in ultra-supercritical power plants, as well as corrosion resistant X2CrNiMo17-12-2 steel was studied in this work. Oxidation tests were carried out under thermal shock conditions in an oxygen-rich environment (containing 50 vol. % water vapor) at a temperature equal to 750 °C. The investigated steels (excluding X2CrNiMo17-12-2 steel) are characterized by good oxidation resistance under thermal shock conditions. A highly protective Cr_2O_3 layer was formed in the internal part of scales growing on the surfaces of investigated steels. The X2CrNiMo17-12-2 steel has worse oxidation resistant properties than the other grades of steels.

Keywords: oxidation, thermal shocks, water vapor, austenitic steels

PACS® (2010). 81.65.Mq – oxidation

Introduction

The global demand for energy has increased rapidly in the last few decades. Such a situation is the result of improving life standards, the increasing number of world population and fast industrialization of underdeveloped countries. According to the most reliable predictions, the energy consumption in 2030 will increase twofold compared to the year 2000 [1, 2]. This will inevitably lead to an energy crisis. Therefore, scientists are obligated, on the other hand, to intensively study the application of alternative energy sources and, on the other hand, to improve the efficiency of currently used power plants [3].

It should be noted that, at present, coal is the dominant source used to fulfill the global primary energy demand [4] and it is obvious that in the near future coal will still be the major source for energy production despite increased utilization of alternative renewable energy sources [5]. Unfortunately, coal plants are the world's largest source of carbon dioxide emissions, which is the primary cause of global warming. Burning coal is also a source of smog, acid rain and toxic air pollution. As a consequence, one of the goals of the power industry is to reduce of pollutant emissions from coal-fired electric generating plants and improve their thermal efficiency. One of the methods that allows for this goal to be achieved is to increase the temperature of steam to about 700 °C in the next 30 years [6]. Unfortunately, ferritic or martensitic steels, commonly used in coal plants, do not have sufficient mechanical properties in these conditions. It has been confirmed that new grades of steels that have been elaborated up to now (e. g. TP91, TP92, etc.) exhibit good creep resistance. However their corrosion resistance is not satisfactory at temperatures higher than 550 °C in the presence of water vapor. In addition, the degradation mechanism of these steels has not yet been fully explained, because of its high complexity, which is mainly the result of the complex chemistry of combustion gases containing water vapor. Consequently, great effort has been made in many scientific centers across the world to select a group of high-temperature materials resistant against oxidation in the temperature range 700–750 °C, which could be applied in coal-fired power plants [7–13]. The oxidation resistance of these materials depends, first of all, on chromium concentration, which should be high enough for selective chromium oxidation and the formation of a highly protective chromia scale (Cr_2O_3) well adherent to the substrate. In spite of this effort, however, there is still a lack of adequate materials.

***Corresponding author: Grzegorz Smola,** Department of Physical Chemistry and Modelling, Faculty of Materials Science and Ceramics, AGH University of Science and Technology, Krakow, Poland, E-mail: smola@agh.edu.pl
Barbara Koscielniak, Department of Materials Science and Metallurgy, Silesian University of Technology, Katowice, Poland
Zbigniew Grzesik, Department of Physical Chemistry and Modelling, Faculty of Materials Science and Ceramics, AGH University of Science and Technology, Krakow, Poland
Adam Hernas, Department of Materials Science and Metallurgy, Silesian University of Technology, Katowice, Poland

Thus, the aim of the present work was to obtain preliminary information about the oxidation resistance under thermal shock conditions in an environment containing water vapor of a number of heat resistant chromium-nickel austenitic steels, which can potentially be used in ultra-supercritical power plants, operating in the temperature range 700–750 °C. The materials selected for research in this work are presently used in incineration and biomass-fired boilers at temperatures not exceeding 600 °C. However, their behavior at higher temperatures has not been systematically tested.

Materials and experimental procedure

Five chromium-nickel austenitic steels (X2CrNiMo17-12-2; Sanicro 25; HR3C; HR6W; Super 304 H) have been selected for investigation. Their chemical composition is summarized in Table 1. Rectangular samples for corrosion experiments, with surface areas of about 6 cm^2 and thickness equal to 1 mm, have been cut from the previously mentioned materials. These samples were grinded with emery papers (up 800 SiC) and degreased in alcohol with the use of an ultrasonic cleaner and then dried in air directly before oxidation tests. Oxidation tests under thermal shock conditions were carried out in an oxygen atmosphere, containing 50 vol. % of water vapor in the apparatus presented schematically in Figure 1.

The realization of corrosion tests under thermal shock conditions requires a short explanation. It should be noted, namely, that boilers in coal plants do not operate under strictly isothermal conditions. During breaks in their operating procedure, boilers are cooled down and then rapidly heated to their working temperature. It is well known that high thermal stresses in such a case develop in the scale-substrate system due to different thermal expansion coefficients of both materials [14, 15] and consequently, during heating and cooling, cracking and spalling of the scale is observed, which considerably lowers the oxidation resistance of the utilized materials [16, 17].

The oxidation studies carried out in this work consisted of rapid heating of a given sample located in the

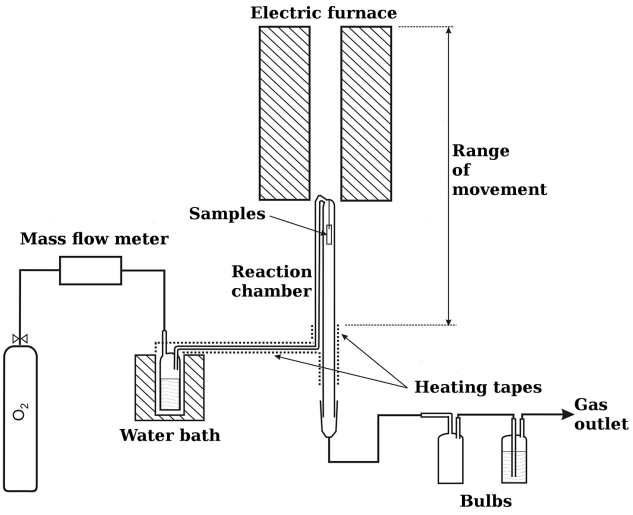

Figure 1: Scheme of the apparatus for oxidation test of metals in an atmosphere containing steam under thermal shocks conditions.

Table 1: Chemical composition of tested materials (mass %).

Material	Chemical composition							
	C	Ni	Cr	Si	Nb	Mn	Fe	Another
X2CrNiMo17-12-2	max 0.03	10.0–13.0	16.5–18.5	max 1.0		max 2.0	bal.	Mo: 2.0–2.5
Sanicro 25	≤ 0.1	25	22.5	0.2	0.5	0.5	bal.	W: 3.6 Co: 1.5 Cu: 3.0 N: 0.23
Super 304H	0.07–0.13	7.5–10.0	17.0–19.0	max 0.3	0.3–0.6	max 1.0	bal.	Cu: 2.5–3.5 N: 0.05–0.12
HR3C	0.04–0.10	17.0–23.0	24.0–26.0	max 0.75	0.2–0.6	max 2.0	bal.	N: 0.15–0.35
HR6W	0.10	bal.	21.5–24.5	1.0	0.1–0.35	1.5	20–27	Ti: 0.05–0.2 W: 6.0–8.0 B: 0.0005-0.0006

reaction chamber of the apparatus shown in Figure 1 from room temperature to 750 °C. The sample was then treated at this temperature for two hours and subsequently cooled down rapidly (quenching) to room temperature. The duration of the heating time was approximately equal to 1 min. The cooling (quenching) time, in turn, proceeded in air atmosphere for about 2 min. These experiments were performed to determine the mass changes of corroded samples as a function of the number of thermal shocks. Mass changes of the investigated materials were determined once per day using a laboratory balance (Radwag model AS60 with sensitivity equal to 10 μg). The heating temperature equal to 750 °C was chosen to simulate the most sever conditions, currently required in coal-fired boilers with supercritical parameters and the number of applied thermal shocks, equal to 100, is comparable with the average number of operating breaks of coal-fired boilers during their lifetime in the power industry.

The interpretation of the conducted corrosion tests is as follows. If corroded samples gradually lose their masses as the number of successive thermal shocks increases, it denotes that formed scales crack and spall off from oxidized materials due to thermal stresses. From these experiments it follows that the higher the mass losses of a given sample are, the worse the scale adherence and protective properties of the scale. On the other hand, if the mass of the sample does not virtually change as the number of shocks increases, it means that in spite of thermal stresses generated in the scale-metallic core system, the scale does not crack and spall off from the substrate surface due to its very good adherence. Consequently, such a scale satisfactorily protects the oxidized material against high temperature corrosion.

After terminating the oxidation tests, scale morphology was examined via an optical microscope (Olympus GX71), as well as a scanning electron microscope (Hitachi S-4200). Chemical composition analysis of the oxidation products was performed using SEM-coupled with a X-ray energy dispersive spectrometer (EDS) Thermo NORAN (System Seven). The phase composition of the scales was studied by the electron backscatter diffraction (EBSD) technique. EBSD analysis was performed using standard conditions for this method, i. e. accelerating voltage of 20 KeV, fixed glancing angle of 70 ° and distance between detector and sample equal to 20 mm. The penetration depth of the electron beam was in the range 25 μm. Crystalline structures in selected micro-regions were identified using INCA HKL Nordlys II with Channel 5 software.

Results and discussion

The results of thermal shock experiments carried out in an oxygen-rich atmosphere containing 50 % of water vapor are presented in Figure 2.

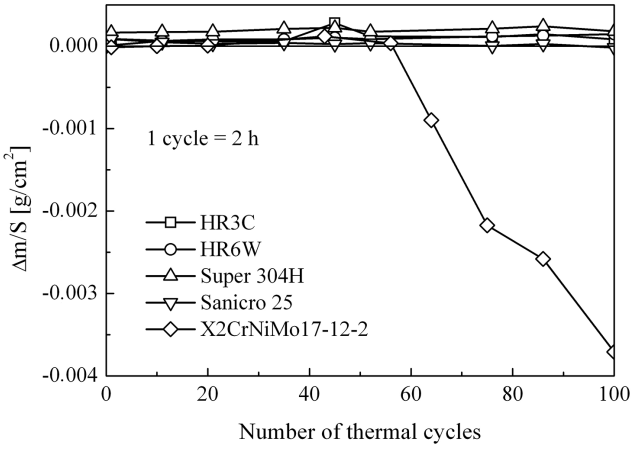

Figure 2: The results of thermal shocks of all materials under investigation (Δm/S – mass changes of the oxidized samples per unit surface area).

From this Figure it follows that data obtained for all studied materials do not significantly differ. In fact, the masses of all studied samples, excluding the X2CrNiMo 17-12-2 steel sample, are virtually constant. This means that the adherence of growing scales to steel surfaces is very good. In the case of all these steels, excluding X2CrNiMo17-12-2 steel, the scales were compact, well adherent to the metallic core and did not spall off from the samples. These conclusions based on kinetic results were in full agreement with the morphological observations described below. On the other hand, the X2CrNiMo 17-12-2 steel sample starts to lose its mass after about 50 thermal shocks. Mass losses are not high, but they denote that adherence of scale to the X2CrNiMo 17-12-2 steel is worse compared to those observed for all other materials in this work.

Kinetic results presented in Figure 2 remain in good agreement with observations of scales of oxidized materials. It has been found, namely, that in the case of the X2CrNiMo17-12-2 steel, scale spallation can be easily observed (Figure 3). It should be noted that not the entire scale but only its external layer falls off (Figure 3(b)). Such a situation is the result of different thermal expansion coefficients of Fe_3O_4 (1.5×10^{-5} K^{-1}) [18] and Cr_2O_3 (5.86×10^{-6} K^{-1}) [19] oxides, which form the external and internal part of the oxide scale, respectively. A

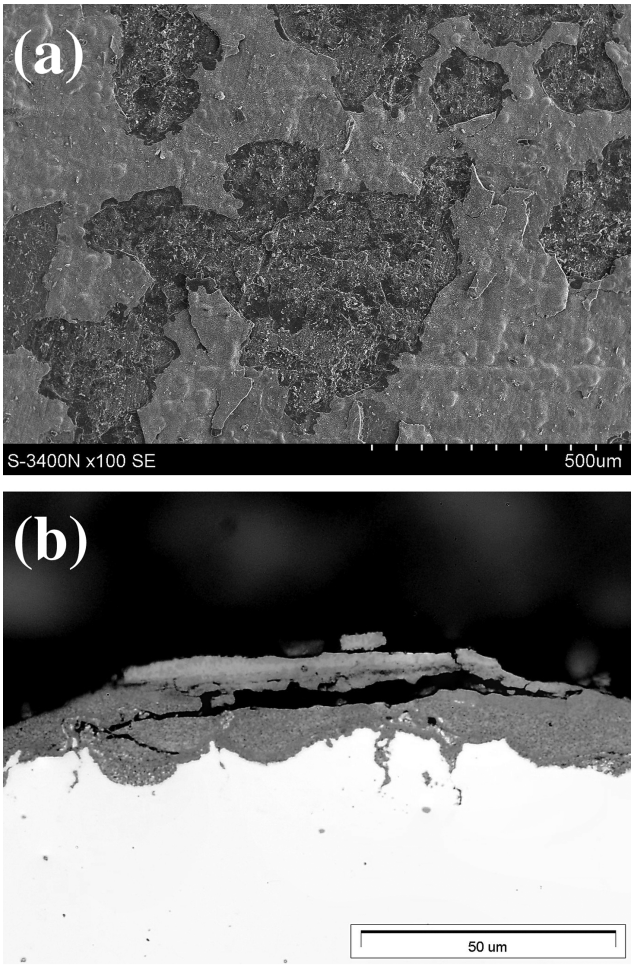

Figure 3: Morphology of the scale formed on the X2CrNiMo17-12-2 steel during oxidation under thermal shock conditions: (a) scale surface (b) cross-section of oxidized sample.

continuous and compact Cr_2O_3 protective layer forms on materials consisting of at least 20 mass % Cr. In this case, the layer constitutes a barrier against outward iron diffusion. Therefore, as a rule, the formation of Fe_3O_4 is not observed on these materials. X2CrNiMo17-12-2 steel consists of 16.5–18.5 mass % chromium, i. e. the lowest amount of that element among the studied steels. Thus, it is impossible for a continuous Cr_2O_3 layer that blocks outward Fe diffusion to form. As a consequence, the presence of Fe_3O_4 is observed on this steel. The formation of Fe_3O_4 is also assisted by a relatively small (compared to the remaining types of steel) amount of nickel, an element which increases Cr diffusion in the steel and thereby facilitates the formation of a continuous Cr_2O_3 layer. The X2CrNiMo17-12-2 steel also contains a relatively large amount of manganese, the influence of which on the formation of Cr_2O_3 is opposite to that of nickel. In contrast to results obtained for this steel, adherence of scales growing on all other materials is much better and no cracking or spallation are observed. In order to illustrate such a situation, in Figure 4 images of the scale surface and cross-section of oxidized Super 304H steel are presented.

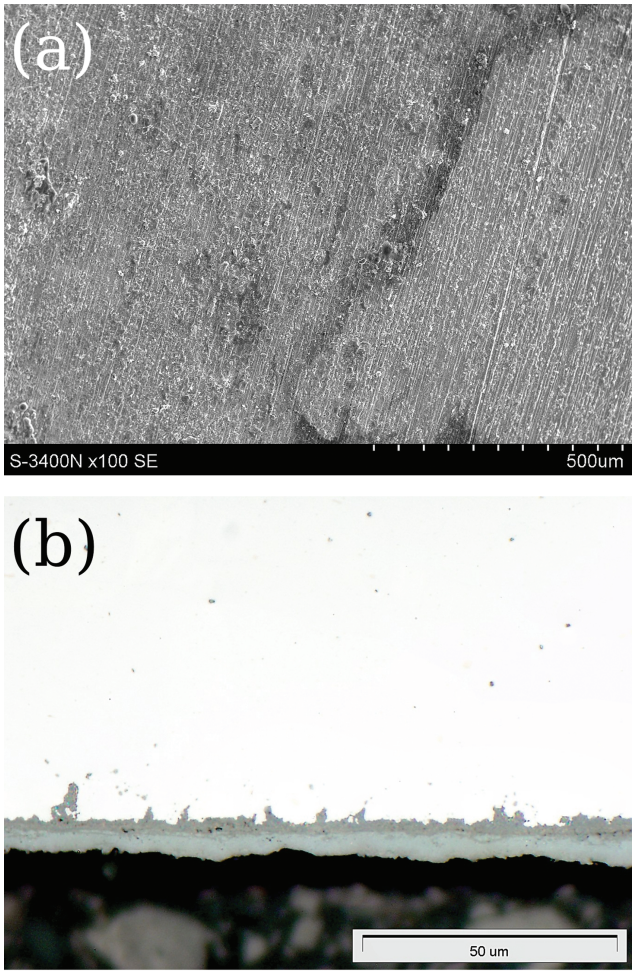

Figure 4: Morphology of the scale formed on the Super 304H steel during oxidation under thermal shock conditions: (a) scale surface (b) cross-section of oxidized sample.

All the studied steels exhibit very good resistance against oxidation under thermal shock conditions and the X2CrNiMo17-12-2 steel exhibits relatively good resistance due to advantageous phase composition of scales growing on the surface of investigated materials. Using the EBSD technique it has been found, namely, that the internal part of the scales growing on all studied steels is composed of highly protective Cr_2O_3 chromium oxide. For illustration, the results obtained during investigation of the internal part of the scales formed on the surfaces of the X2CrNiMo17-12-2 and Super 304H steels are presented in

Figures 5 and 6, respectively. The diffraction analysis of back scattered electrons has been carried out in micro-regions presented in Figures 5(a) and 6(a). Obtained images of Kikuchi lines are shown in Figures 5(b) and 6 (b). The crystalline structure in selected micro-regions, identified using INCA HKL Nordlys II with Channel 5 software, corresponds to Cr_2O_3 oxide, Figures 5(c) and 6(c).

The detailed EBSD analysis of oxidized X2CrNiMo17-12-2 steel samples indicates that in the internal part of the scale, in addition to Cr_2O_3 oxide, the (Cr, Mn, Fe)O_4 phase is also present (Figure 7). Both these oxides are covered by $FeCr_2O_4$, (Figure 8), on the surface of which Fe_3O_4 is formed (Figure 9).

EBSD analysis of scales growing on the Super 304H, HR6W and Sanicro 25 steels shows that these scales are composed only of Cr_2O_3 oxide. In the case of the HR3C steel, the scale contains two crystalline phases: Cr_2O_3 and $(Fe,Cr)_3O_4$. Details of the phase compositions of scales growing on the investigated steels are summarized in Figure 10. It can be seen in Figure 10 that the Cr_2O_3 oxide scale grown on Sannicro 25 steel is compact and continuous. The same result was obtained for all Sanicro 25 steel samples.

As already mentioned, all the studied steels exhibit very good resistance as a result of the formation of highly protective Cr_2O_3 oxide within the scales growing on the surfaces of these steels. However, in spite of this fact, the protective properties of the scale growing on the X2CrNiMo17-12-2 steel are worse than those observed for all other materials in this work. As can be seen in Figure 10, in the case of the X2CrNiMo17-12-2 steel, the thickness of the oxidation product layer formed above Cr_2O_3 oxide is at least one order of magnitude higher than that recorded for other steels. This means that the Cr_2O_3 layer growing on the surface of the X2CrNiMo17-12-2 steel does not constitute as good a barrier for outward diffusion of iron and manganese, as the analogous layers observed in the case of the remaining steels. Thus, the question arises: what is the reason for such a situation?

First of all, it should be mentioned that the investigated steels have different chemical compositions (see Table 1) and, as a consequence, various protective properties of Cr_2O_3 oxide can be a result of the dopping effect. It should be noted, however, that thermal shock tests were conducted at a relatively low temperature, constituting about 38 % of the Cr_2O_3 melting point. Experiments were then carried out at a temperature lower than Tammann's temperature for Cr_2O_3. This means that the dopping effect according to the Hauffe-Wagner theory of

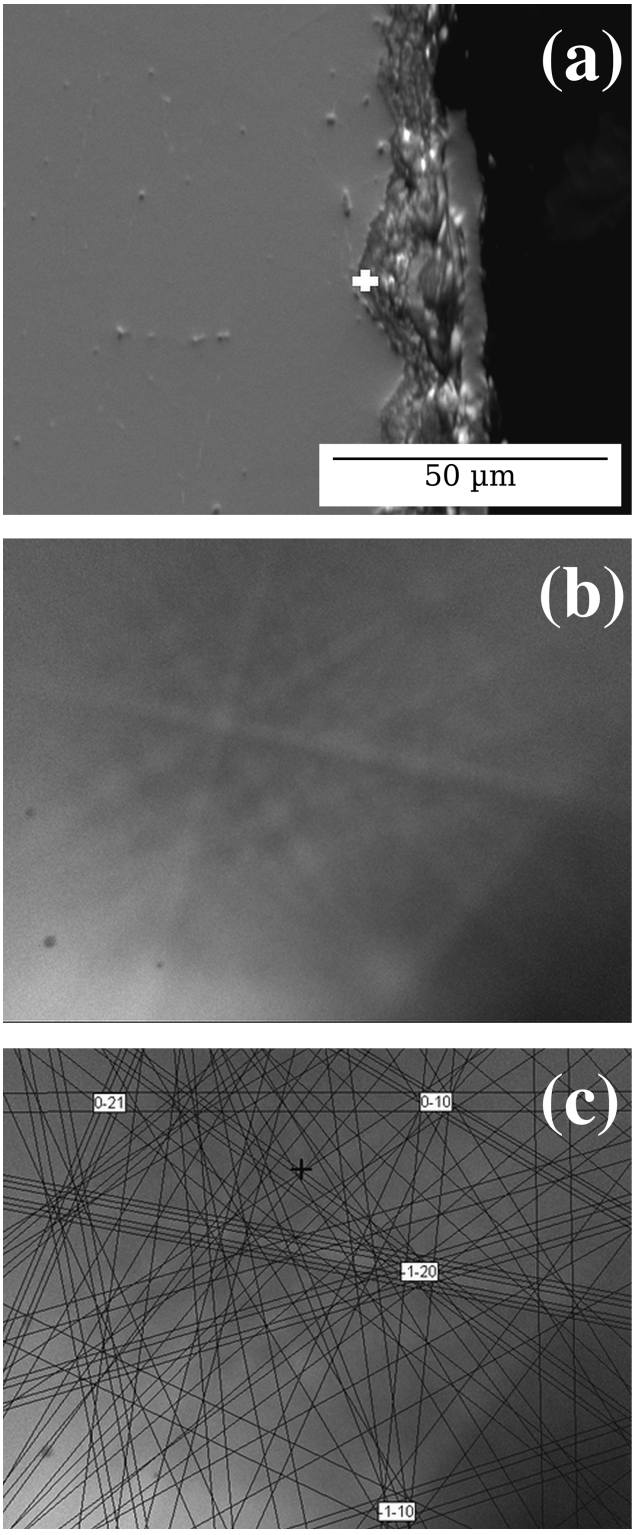

Figure 5: The results of EBSD analysis of the internal part of the oxide scale growing on the surface of the X2CrNiMo17-12-2 steel sample: (a) cross-section of oxidized steel sample with marked micro-region, in which the EBSD analysis has been performed (b) an electron backscatter diffraction pattern (c) results of simulation of indexed planes for crystalline Cr_2O_3.

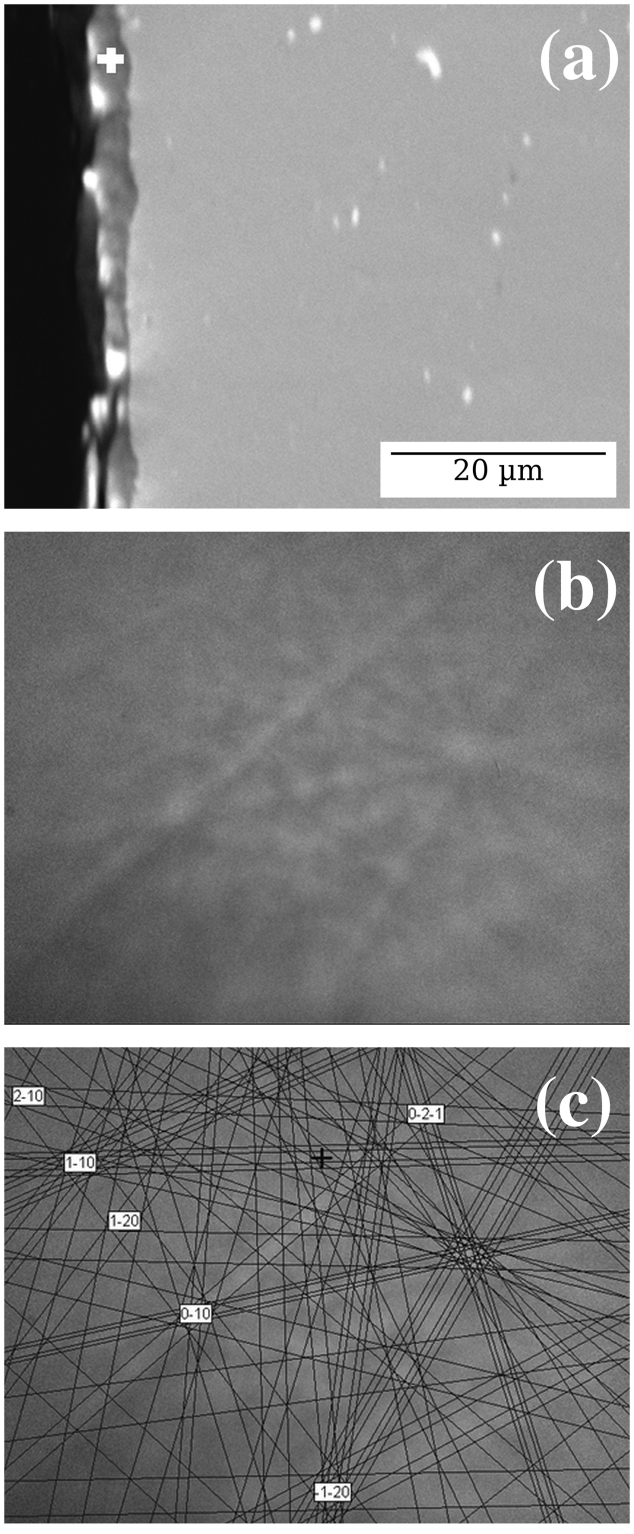

Figure 6: The results of EBSD analysis of the internal part of the oxide scale growing on the surface of the Super 304H steel sample: (a) cross-section of oxidized steel sample with marked micro-region, in which the EBSD analysis has been performed (b) an electron backscatter diffraction pattern (c) results of simulation of indexed planes for crystalline Cr_2O_3.

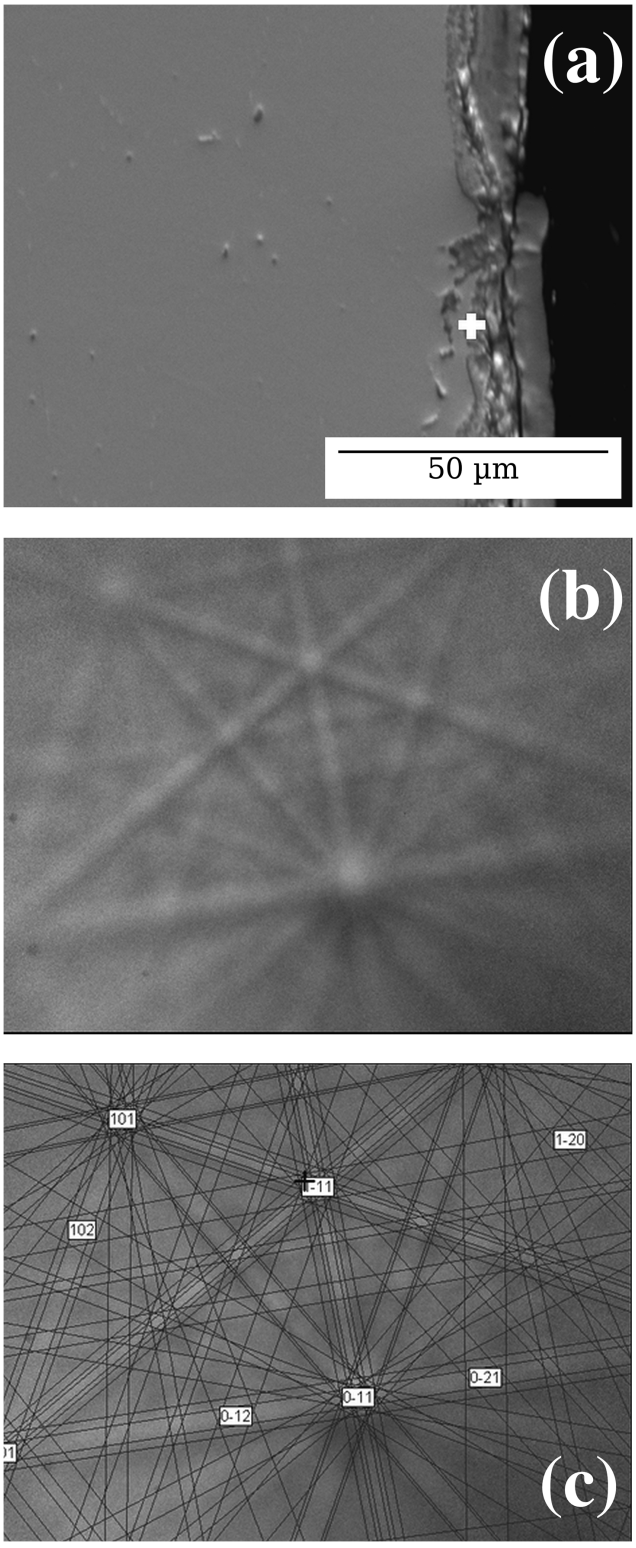

Figure 7: The results of EBSD analysis of the internal part of the oxide scale growing on the surface of the X2CrNiMo17-12-2 steel sample: (a) cross-section of oxidized steel sample with marked micro-region, in which the EBSD analysis has been performed (b) an electron backscatter diffraction pattern (c) results of simulation of indexed planes for crystalline (Cr, Mn, Fe)O_4.

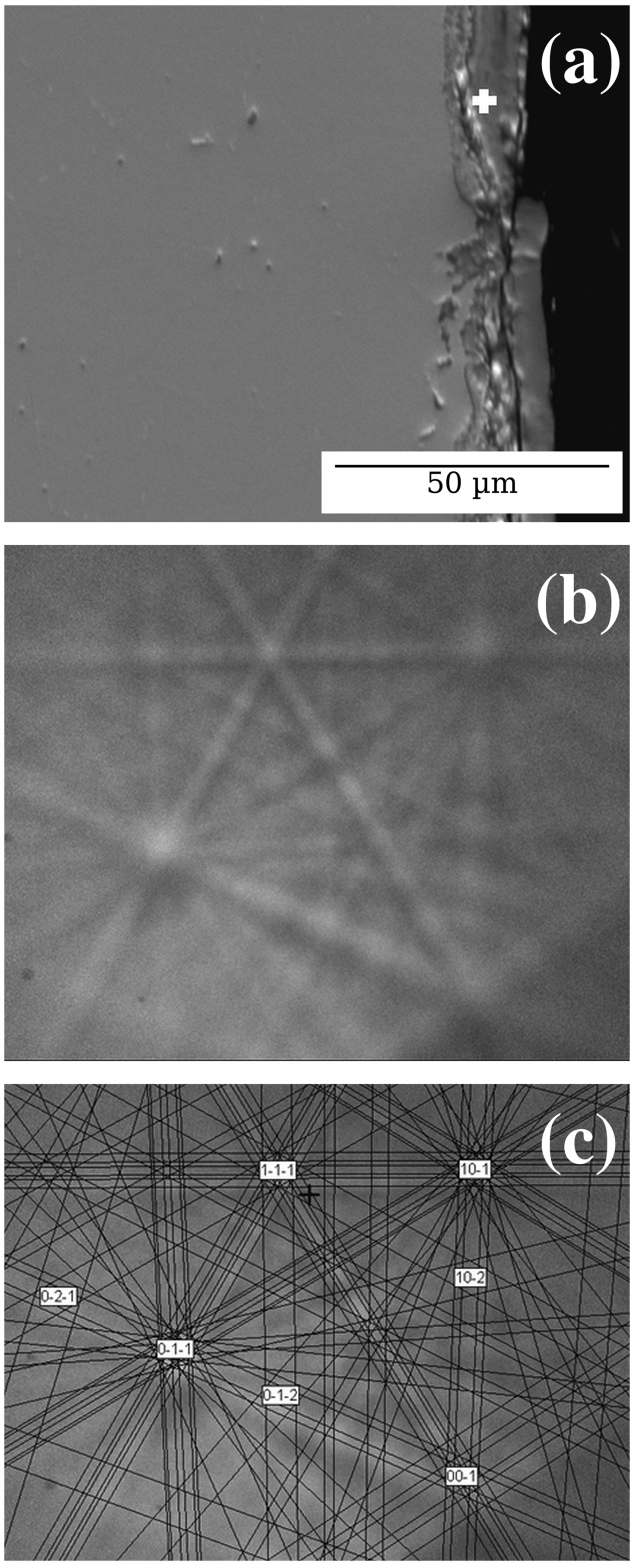

Figure 8: The results of EBSD analysis of the central part of the oxide scale growing on the surface of the X2CrNiMo17-12-2 steel sample: (a) cross-section of oxidized steel sample with marked micro-region, in which the EBSD analysis has been performed (b) an electron backscatter diffraction pattern (c) results of simulation of indexed planes for crystalline $FeCr_2O_4$.

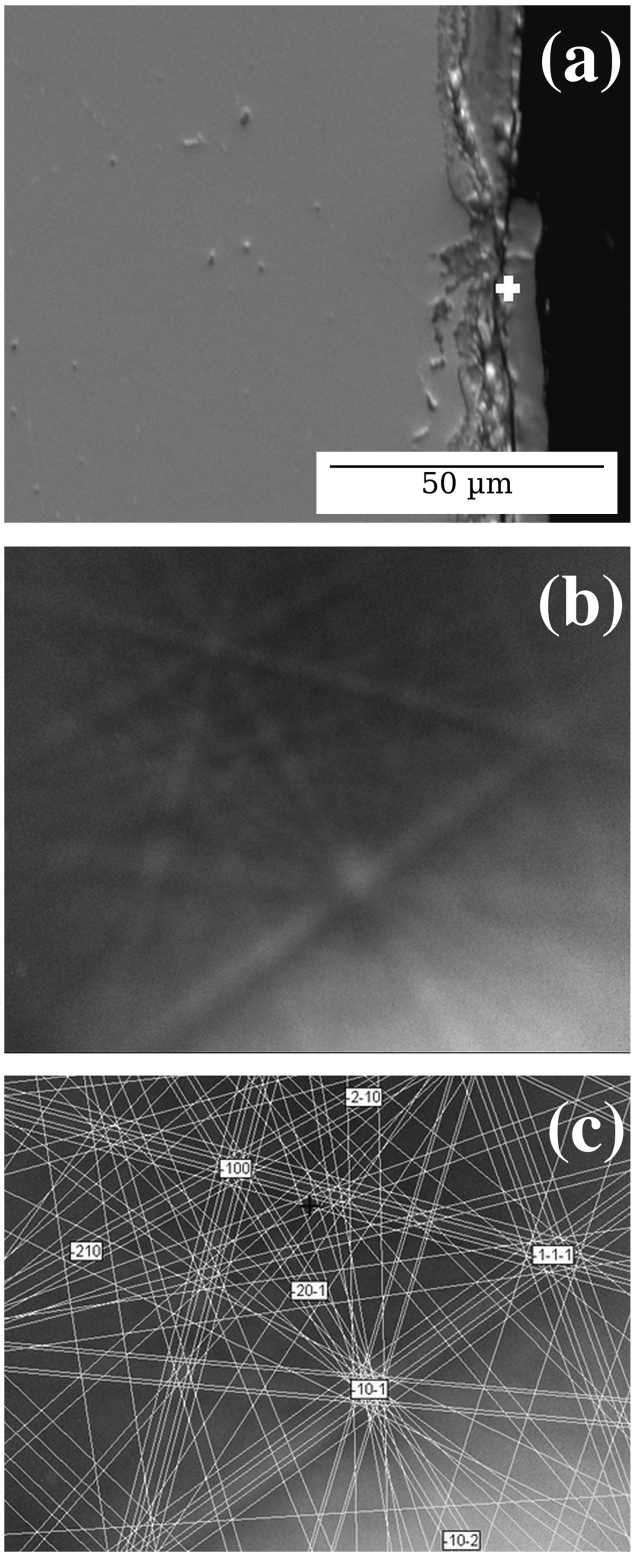

Figure 9: The results of EBSD analysis of the external part of the oxide scale growing on the surface of the X2CrNiMo17-12-2 steel sample (a) cross-section of oxidized steel sample with marked micro-region, in which the EBSD analysis has been performed (b) an electron backscatter diffraction pattern (c) results of simulation of indexed planes for crystalline Fe_3O_4.

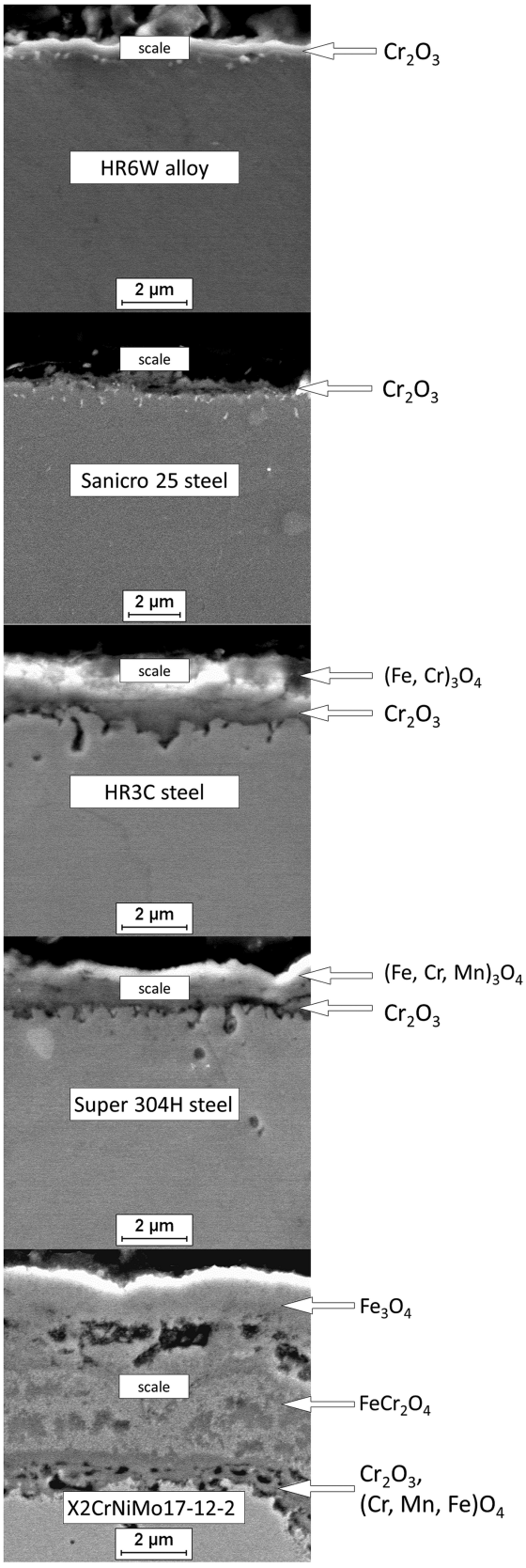

Figure 10: Cross-sections of oxidized materials with marked phases constituting growing scales.

doping [20] cannot be responsible for the higher oxidation rate of the X2CrNiMo17-12-2 steel.

On the other hand, relatively fast outward diffusion of iron and manganese under the applied experimental conditions could proceed via short circuit diffusion paths, such as dislocations or grain boundaries. It has been recently reported that a Cr_2O_3 oxide layer, formed in conditions analogous to those applied in this work, has an extremely fine-grained structure [21]. This fine crystalline Cr_2O_3 oxide layer thereby exhibits a relatively low concentration of dislocations and a very large density of grain boundaries. As a consequence, it can be concluded that grain boundary diffusion should be responsible for the relatively fast degradation rate of the X2CrNiMo17-12-2 steel. In the case of scales formed on the surface of the X2CrNiMo17-12-2 steel samples, the internal scale layer is not only composed of Cr_2O_3, but consists of two oxide phases: Cr_2O_3 and (Cr, Mn, Fe)O_4 (see Figure 7). As the protective properties of oxide spinel phases containing iron are generally worse compared to those of pure Cr_2O_3, the presence of the (Cr, Mn, Fe)O_4 oxide may increase the outward grain boundary diffusion of iron and manganese through the internal layer of the oxide scale on the X2CrNiMo17-12-2 steel.

It should be mentioned, that the presence of the (Cr, Mn, Fe)O_4 oxide in the internal part of scale is not the only potentially possible explanation of the faster degradation rate of the X2CrNiMo17-12-2 steel. In spite of the phase composition results obtained by EBSD and presented in Figure 10, the detailed chemical analysis of scales performed using EDS clearly indicates, namely, that the internal layer of the scales formed on all studied steels is enriched in iron. For illustration, some of the obtained results using the EDS technique are presented in Figure 11. The amount of iron in the internal part of the

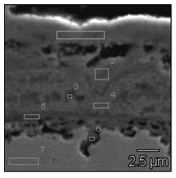

	Si-K	Cr-K	Mn-K	Fe-K	Ni-K	Mo-L
pt1	2.9	18.9	1.1	64.5	11.8	0.8
pt2	2.9	33.1	1.9	40.6	19.4	2.2
pt3	2.7	38.3	2.3	41.9	12.7	2.1
pt4	2.2	31.5	2.3	33.3	28.6	2.0
pt5	2.9	59.3	1.0	31.7	3.2	1.8
pt6	5.4	41.7	3.1	34.8	13.4	1.6
pt7	1.1	18.8	1.6	67.0	10.4	1.0

X2CrNiMo17-12-2

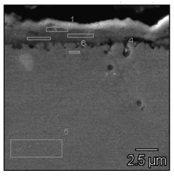

	Si-K	S-K	Cr-K	Mn-K	Fe-K	Ni-K	Cu-K
pt1	4.8		37.9	2.9	54.3		
pt2	3.1		72.7	4.3	20.0		
pt3	1.5	0.4	72.4	2.5	23.1		
pt4	3.6		15.2	0.5	69.5	9.4	1.7
pt5	0.8		20.1	0.7	68.4	7.9	2.1
pt6	0.9	0.4	14.3		70.6	10.4	3.4

Super 304H

Figure 11: Microphotographs of cross-sections of oxidized steel samples with marked regions in which the EDS analysis has been performed and the results of such analysis (expressed in at. %).

scale growing on the X2CrNiMo17-12-2 steel reaches about 32 at.%, while in the case of other steels it changes in the range of 3–20 at. %. These values are too high to be a result of experimental error and the lack of oxide phases containing iron at the steel-scale interface should be explained. It is relatively easy to explain such a situation in the case of the X2CrNiMo17-12-2 steel, due to the presence of the (Cr, Mn, Fe)O_4 oxide in internal part of the scale. However, according to EBSD analysis the internal part of scales formed on all remaining steels was composed only of Cr_2O_3. This apparent disagreement in the results obtained using EBSD and EDS methods can be explained as being caused by the presence of glassy oxide phases. Using the EBSD technique, crystalline oxide phases have been detected, while EDS analysis can give information about the chemical composition of crystalline and amorphous phases. The possibility of glassy phases formation in the internal part of the scales growing on Sanicro 25 steel has been recently reported [21]. As the diffusion rate in crystalline and amorphous materials can differ significantly, the presence of non-crystalline oxide phases in investigated scales can be potentially treated as an important factor that increases the diffusion rate of reactants. The influence of the presence of (Cr, Mn, Fe)O_4 oxide, grain boundaries, as well as glassy phases in formed oxide scales on the degradation rate of investigated steels requires further detailed studies. It should be noted that all investigated materials are austenitic steels, which means that the size and distribution of the grains were comparable in each case. Therefore, the different oxidation rates of the individual steels should not be caused by the microstructures of these steels, but by their different chemical compositions.

Conclusions

One of the most important conclusions, resulting from this work is that all steels under investigation have good resistant properties under thermal shock conditions. This is due to the formation of a highly protective Cr_2O_3 layer in scales growing on the surfaces of studied steels. It has been demonstrated, however, that the X2CrNiMo17-12-2 steel has the lowest oxidation resistance among all the studied materials. The relatively fast degradation rate of this steel was tentatively explained as a result of the presence of short circuit diffusion paths in (Cr, Mn, Fe)O_4 oxide, which was detected only in the internal part of the scales growing on the X2CrNiMo17-12-2 steel. From a practical point of view, it may be then concluded that coal-fired boilers in ultra-supercritical power plants should not be manufactured in the future using the X2CrNiMo17-12-2 steel.

Funding: The results presented in this paper were obtained in the research work co-financed by the National Centre of Research and Development in the framework of contract PBS2/B4/8/2013 – Programme of Applied Research, PBSII: DUO-BIO – Low-carbon innovative technologies for modernization of 200 MW coal-fired power units.

References

[1] C.N. Hamelinck and A.P.C. Faaij, Energy Policy, 34 (2006) 3268–3283.
[2] R. Gilbert and A. Perl, Energy and transport futures. A report prepared for national round table on the environment and the economy, University of Calgary, June 2005, 1–96.
[3] P.J. Ennis, Advances in Material Technology for Fossil Power Plants, ASM International, London (2001), pp. 187–196.
[4] E. Kakaras, A. Koumanakos, A. Doukelis, D. Giannakopoulos and I. Vorrias, Fuel, 86 (2007) 2144–2150.
[5] K. Natesan and Z. Zeng, Adv. Sci. Technol., 72 (2010) 1–11.
[6] R. Viswanathan and W. Bakker, J. Mater. Eng. Perform., 10 (1) (2001) 81–95.
[7] A.J. Bennett and P.S. Weitzel, Boiler materials for ultrasupercritical coal power plants – Task 1B, Conceptual Design, Babcock & Wilcox Approach, USC T-3, Topical Report, DOE DE-FG26-01NT41175 & OCDO D-0020, February (2003).
[8] G. Booras, Task 1C, Economic Analysis, Boiler materials for ultra-supercritical coal power plants, DOE Grant DE-FG26-01NT41175, OCDO Grant D-00-20, Topical Report USC T-1, February (2003).
[9] R. Viswanathan, J. Shingledecker and J. Phillips, Pursuit of efficiency in coal power plants (ed. B.A. Sakrestad), 35th International Technical Conference on Clean Coal and Fuel Systems 2010, Clearwater, FL, June (2010).
[10] J.P. Schingledecker, B. Pint, A.S. Sabau, A.T. Fry and I.G. Wright, Adv. Mater. Process., 171 (2013) 23–25.
[11] H.G. Simms, Oxidation behaviour of austenitic stainless steels at high temperature in supercritical plant, M.Res. thesis, University of Birmingham (2011).
[12] V.F.C. Lins, M.M.R. Castro, R.Z. Domingues and T. Matencio, Chem. Eng. Technol., 33 (2010) 354–360.
[13] R. Peraldi and B.A. Pint, Oxid. Met., 61 (2004) 463–483.
[14] S. Mrowec and T. Werber, Modern Scaling-Resistant Materials, National Bureau of Standards and National Science Foundation, Washington, DC (1982).
[15] P. Kofstad, High Temperature Corrosion, Elsevier Applied Science, London and New York (1988).

[16] D. Naumenko, L. Singheiser and W.J. Quadakkers, Oxidation limited of FeCrAl based alloys during thermal cyclic, in Proc. EFC Workshop, Frankfurt/Main (1999) p. 287.
[17] M. Beukenberg, Thermal fatigue evaluation of EB-PVD TBCs with different bond coats, in Proc. Turbine Forum 2006, Advances Coatings for High Temperatures, Nice, April (2006) pp. 26–28.
[18] M. Takeda, T. Onishi, S. Nakakubo and S. Fujimoto, Mater. Trans., 50 (2009) 2242–2246.
[19] H.P. Kirchner, Prog. Solid State Chem., 1 (1964) 1–36.
[20] K. Hauffe, Reaktionen in Und an Festen Stoffen, Springer, Berlin (1955).
[21] B. Rutkowskia, A. Gil and A. Czyrska-Filemonowicz, Corros. Sci. 102 (2016) 373–383.